Characterization of broadband few-cycle laser pulses with the d-scan technique

Miranda, Miguel; Arnold, Cord; Fordell, Thomas; Silva, Francisco; Alonso, Benjamin; Weigand, Rosa; L'Huillier, Anne; Crespo, Helder

Published in:
Optics Express

DOI:
10.1364/OE.20.018732

2012

Characterization of broadband few-cycle laser pulses with the d-scan technique

Miguel Miranda,[1,2,*] Cord L. Arnold,[2] Thomas Fordell,[2] Francisco Silva,[1] Benjamín Alonso,[3] Rosa Weigand,[4] Anne L'Huillier,[2] and Helder Crespo[1]

[1]*IFIMUP-IN and Departamento de Física e Astronomia, Universidade do Porto, Rua do Campo Alegre 687, 4169-007 Porto, Portugal*

[2]*Department of Physics, Lund University, P.O. Box 118, SE-221 00 Lund, Sweden*

[3]*Grupo de Investigación en Óptica Extrema (GIOE), Universidad de Salamanca, Pl. de la Merced s/n, E-37008 Salamanca, Spain*

[4]*Departamento de Óptica, Facultad de Ciencias Físicas, Universidad Complutense de Madrid, Avda. Complutense s/n, 28040 Madrid, Spain*

[*]*mmiranda@fc.up.pt*

Abstract: We present an analysis and demonstration of few-cycle ultrashort laser pulse characterization using second-harmonic dispersion scans and numerical phase retrieval algorithms. The sensitivity and robustness of this technique with respect to noise, measurement bandwidth and complexity of the measured pulses is discussed through numerical examples and experimental results. Using this technique, we successfully demonstrate the characterization of few-cycle pulses with complex and structured spectra generated from a broadband ultrafast laser oscillator and a high-energy hollow fiber compressor.

OCIS codes: (320.2250) Femtosecond phenomena; (320.5520) Pulse compression; (320.7090) Ultrafast lasers; (320.7100) Ultrafast measurements.

References and links

1. U. Morgner, R. Ell, G. Metzler, T. R. Schibli, F. X. Kärtner, J. G. Fujimoto, H. A. Haus, and E. P. Ippen, "Nonlinear Optics with Phase-Controlled Pulses in the Sub-Two-Cycle Regime," Phys. Rev. Lett. **86**(24), 5462–5465 (2001).
2. S. Rausch, T. Binhammer, A. Harth, J. Kim, R. Ell, F. X. Kärtner, and U. Morgner, "Controlled waveforms on the single-cycle scale from a femtosecond oscillator," Opt. Express **16**(13), 9739–9745 (2008).
3. T. Fuji, A. Unterhuber, V. S. Yakovlev, G. Tempea, A. Stingl, F. Krausz, and W. Drexler, "Generation of smooth, ultra-broadband spectra directly from a prism-less Ti:sapphire laser," Appl. Phys. B **77**(1), 125–128 (2003).
4. H. M. Crespo, J. R. Birge, E. L. Falcão-Filho, M. Y. Sander, A. Benedick, and F. X. Kärtner, "Nonintrusive phase stabilization of sub-two-cycle pulses from a prismless octave-spanning Ti:sapphire laser," Opt. Lett. **33**(8), 833–835 (2008).
5. A. Dubietis, G. Jonušauskas, and A. Piskarskas, "Powerful femtosecond pulse generation by chirped and stretched pulse parametric amplification in BBO crystal," Opt. Commun. **88**(4-6), 437–440 (1992).
6. A. Dubietis, R. Butkus, and A. P. Piskarskas, "Trends in chirped pulse optical parametric amplification," IEEE J. Sel. Top. Quantum Electron. **12**(2), 163–172 (2006).
7. D. Strickland and G. Mourou, "Compression of amplified chirped optical pulses," Opt. Commun. **56**(3), 219–221 (1985).
8. A. Amani Eilanlou, Y. Nabekawa, K. L. Ishikawa, H. Takahashi, and K. Midorikawa, "Direct amplification of terawatt sub-10-fs pulses in a CPA system of Ti:sapphire laser," Opt. Express **16**(17), 13431–13438 (2008).
9. F. Krausz and M. Ivanov, "Attosecond physics," Rev. Mod. Phys. **81**(1), 163–234 (2009).
10. E. Esarey, C. B. Schroeder, and W. P. Leemans, "Physics of laser-driven plasma-based electron accelerators," Rev. Mod. Phys. **81**(3), 1229–1285 (2009).
11. M. Nisoli, S. De Silvestri, and O. Svelto, "Generation of high energy 10 fs pulses by a new pulse compression technique," Appl. Phys. Lett. **68**(20), 2793 (1996).
12. M. Nisoli, S. De Silvestri, O. Svelto, R. Szipöcs, K. Ferencz, Ch. Spielmann, S. Sartania, and F. Krausz, "Compression of high-energy laser pulses below 5 fs," Opt. Lett. **22**(8), 522–524 (1997).
13. C. P. Hauri, W. Kornelis, F. W. Helbing, A. Heinrich, A. Couairon, A. Mysyrowicz, J. Biegert, and U. Keller, "Generation of intense, carrier-envelope phase-locked few-cycle laser pulses through filamentation," Appl. Phys. B **79**(6), 673–677 (2004).
14. I. Walmsley and C. Dorrer, "Characterization of ultrashort electromagnetic pulses," Adv. Opt. Photon. **1**(2), 308–437 (2009).

#167354 - $15.00 USD Received 25 Apr 2012; revised 25 May 2012; accepted 12 Jun 2012; published 1 Aug 2012

15. J. C. M. Diels, J. J. Fontaine, I. C. McMichael, and F. Simoni, "Control and measurement of ultrashort pulse shapes (in amplitude and phase) with femtosecond accuracy," Appl. Opt. **24**(9), 1270–1282 (1985).
16. C. Iaconis and I. A. Walmsley, "Spectral phase interferometry for direct electric-field reconstruction of ultrashort optical pulses," Opt. Lett. **23**(10), 792–794 (1998).
17. A. S. Wyatt, I. A. Walmsley, G. Stibenz, and G. Steinmeyer, "Sub-10 fs pulse characterization using spatially encoded arrangement for spectral phase interferometry for direct electric field reconstruction," Opt. Lett. **31**(12), 1914–1916 (2006).
18. J. R. Birge, H. M. Crespo, and F. X. Kärtner, "Theory and design of two-dimensional spectral shearing interferometry for few-cycle pulse measurement," J. Opt. Soc. Am. B **27**(6), 1165–1173 (2010).
19. V. V. Lozovoy, I. Pastirk, and M. Dantus, "Multiphoton intrapulse interference. IV. Ultrashort laser pulse spectral phase characterization and compensation," Opt. Lett. **29**(7), 775–777 (2004).
20. B. Xu, J. M. Gunn, J. M. D. Cruz, V. V. Lozovoy, and M. Dantus, "Quantitative investigation of the multiphoton intrapulse interference phase scan method for simultaneous phase measurement and compensation of femtosecond laser pulses," J. Opt. Soc. Am. B **23**(4), 750–759 (2006).
21. Y. Coello, V. V. Lozovoy, T. C. Gunaratne, B. Xu, I. Borukhovich, C.-H. Tseng, T. Weinacht, and M. Dantus, "Interference without an interferometer: a different approach to measuring, compressing, and shaping ultrashort laser pulses," J. Opt. Soc. Am. B **25**(6), A140–A150 (2008).
22. V. V. Lozovoy, B. Xu, Y. Coello, and M. Dantus, "Direct measurement of spectral phase for ultrashort laser pulses," Opt. Express **16**(2), 592–597 (2008).
23. D. J. Kane and R. Trebino, "Characterization of arbitrary femtosecond pulses using frequency-resolved optical gating," IEEE J. Quantum Electron. **29**(2), 571–579 (1993).
24. R. Trebino and D. J. Kane, "Using phase retrieval to measure the intensity and phase of ultrashort pulses: frequency-resolved optical gating," J. Opt. Soc. Am. A **10**(5), 1101–1111 (1993).
25. R. Trebino, K. W. DeLong, D. N. Fittinghoff, J. N. Sweetser, M. A. Krumbugel, B. A. Richman, and D. J. Kane, "Measuring ultrashort laser pulses in the time-frequency domain using frequency-resolved optical gating," Rev. Sci. Instrum. **68**(9), 3277–3295 (1997).
26. M. Miranda, T. Fordell, C. Arnold, A. L'Huillier, and H. Crespo, "Simultaneous compression and characterization of ultrashort laser pulses using chirped mirrors and glass wedges," Opt. Express **20**(1), 688–697 (2012).
27. D. Keusters, H.-S. Tan, P. O'Shea, E. Zeek, R. Trebino, and W. S. Warren, "Relative-phase ambiguities in measurements of ultrashort pulses with well-separated multiple frequency components," J. Opt. Soc. Am. B **20**(10), 2226–2237 (2003).
28. A. Baltuška, M. S. Pshenichnikov, and D. A. Wiersma, "Amplitude and phase characterization of 4.5-fs pulses by frequency-resolved optical gating," Opt. Lett. **23**(18), 1474–1476 (1998).
29. A. Baltuška, M. S. Pshenichnikov, and D. A. Wiersma, "Second-harmonic generation frequency-resolved optical gating in the single-cycle regime," IEEE J. Quantum Electron. **35**(4), 459–478 (1999).
30. J. A. Nelder and R. Mead, "A simplex method for function minimization," Comput. J. **7**, 308–313 (1965).
31. V. S. Yakovlev, P. Dombi, G. Tempea, C. Lemell, J. Burgdorfer, T. Udem, and A. Apolonski, "Phase-stabilized 4-fs pulses at the full oscillator repetition rate for a photoemission experiment," Appl. Phys. B **76**(3), 329–332 (2003).
32. A. Baltuška, A. Pugzlys, M. S. Pshenichnikov, and D. A. Wiersma, "Rapid amplitude-phase reconstruction of femtosecond pulses from intensity autocorrelation and spectrum," in *Conference on Lasers and Electro-Optics*, 1999 OSA Technical Digest Series (Optical Society of America, Washington, D.C., 1999), 264–265.
33. C. Dorrer and I. Walmsley, "Accuracy criterion for ultrashort pulse characterization techniques: application to spectral phase interferometry for direct electric field reconstruction," J. Opt. Soc. Am. B **19**(5), 1019–1029 (2002).
34. G. Stibenz, C. Ropers, Ch. Lienau, Ch. Warmuth, A. S. Wyatt, I. A. Walmsley, and G. Steinmeyer, "Advanced methods for the characterization of few-cycle light pulses: a comparison," Appl. Phys. B **83**(4), 511–519 (2006).
35. A. S. Wyatt, A. Grün, P. K. Bates, O. Chalus, J. Biegert, and I. A. Walmsley, "Accuracy measurements and improvement for complete characterization of optical pulses from nonlinear processes via multiple spectral-shearing interferometry," Opt. Express **19**(25), 25355–25366 (2011).
36. D. R. Austin, T. Witting, and I. A. Walmsley, "Resolution of the relative phase ambiguity in spectral shearing interferometry of ultrashort pulses," Opt. Lett. **35**(12), 1971–1973 (2010).
37. H. Crespo, M. Miranda, P. Oliveira, and R. Weigand are preparing a manuscript to be called "Broadband 5.9-fs Ti:sapphire laser characterized using the dispersion-scan technique."

1. Introduction

Today's femtosecond laser oscillators can easily deliver pulse durations in the few-cycle regime [1–4]. Ultra-broadband oscillators based on Ti:Sapphire usually operate in regimes where strong nonlinearities occur within the gain medium itself, which can lead to broadband and highly structured spectra. On the other hand, there is a strong demand for high-power ultrashort pulses not achievable directly with laser oscillators. These can be produced by optical parametric chirped pulse amplification (OPCPA) [5, 6] or by chirped pulse amplification (CPA) [7, 8]. It is however a complicated task to preserve the short pulse duration in the amplification process in traditional CPA systems, as effects like gain

#167354 - $15.00 USD Received 25 Apr 2012; revised 25 May 2012; accepted 12 Jun 2012; published 1 Aug 2012

narrowing reduce the spectral width of the amplified pulses. Thus, external pulse compression schemes are usually employed that can provide energetic pulses in the few- to single-cycle regimes. These pulses have become indispensable tools in attoscience [9] and high-field physics [10]. The most common external compression schemes involve spectral broadening of amplified pulses by self phase modulation (SPM), either in a gas-filled capillary waveguide [11, 12] or in a self-guided filament [13], usually followed by temporal compression with chirped mirrors. The resulting spectra are generally a few hundred nanometers wide, often featuring strong modulations and spectral gaps. Furthermore, the phase acquired by the pulses in the broadening process is complicated due to the interplay between several effects, such as SPM, dispersion, plasma generation, and shockwave formation, and in practice can only be partially compensated for by chirped mirrors. Considering the broadband spectra with complicated structure and phase that normally arise, the characterization of pulses delivered by these external compression schemes is usually quite challenging.

When characterizing ultrashort laser pulses, different methods have different strengths and weaknesses [14]. The existing measurement techniques can be broadly defined to operate in the time domain (i.e., autocorrelations [15]), the spectral domain (spectral phase interferometry for direct electric-field reconstruction - SPIDER - and variants [16–18], and multiphoton intrapulse interference phase scan - MIIPS [19–22]) or both domains (frequency resolved optical gating - FROG [23–25]).

We have recently demonstrated a simple technique to characterize ultrashort pulses while compressing them with chirped mirrors and glass wedges [26]. Since chirped mirrors introduce fixed amounts of dispersion, they're commonly used together with a pair of glass wedges to fine-tune the dispersion so as to reach maximum compression. By measuring the fundamental spectrum and the second-harmonic generation (SHG) spectra around this optimum glass insertion, together with a numerical iterative algorithm, it is possible to fully characterize the pulses without the need for further diagnostics. In this work, we investigate the applicability of the method (which we call *d-scan,* short for dispersion scan) to particularly complex cases, namely sources with complex spectra (both in spectral power and phase), as well as its robustness to measurement bandwidth and noise. We demonstrate, via simulations and experiments, that it is possible to reconstruct the phase of few-cycle pulses generated by ultrabroad bandwidth oscillators and from post-compression in a hollow fiber from a CPA system. The main advantages of this technique are its simplicity (ease of alignment), sensitivity (no need for pulse splitting, so it uses all the available energy), relaxed bandwidth requirements, and the ability to measure the relative phase between well separated frequency components, provided the spectral gap between them is smaller than the largest continuous spectral region [27]. The cases considered here (both simulated and experimental) are of particular relevance for state-of-the-art broadband ultrashort pulse sources, where spectra are the result of complex nonlinear processes (e.g., Kerr effect and plasma interaction).

2. Method

An ultrashort laser pulse can be described by its complex spectral amplitude

$$\tilde{U}(\omega) = \left|\tilde{U}(\omega)\right| \exp\{i\,\phi(\omega)\}. \tag{1}$$

If the pulse goes through a piece of transparent glass and then a SHG crystal, the measured SHG spectral power as a function of thickness is proportional to

$$S(\omega, z) = \left| \int \left(\int \tilde{U}(\Omega) \exp\left\{ izk(\Omega) \right\} \exp(i\,\Omega t)\, d\Omega \right)^2 \exp(-i\,\omega t)\, dt \right|^2, \tag{2}$$

which can also be written in the spectral domain as a convolution (as usually found in MIIPS literature [19–22])

#167354 - $15.00 USD Received 25 Apr 2012; revised 25 May 2012; accepted 12 Jun 2012; published 1 Aug 2012

$$S(\omega,z)=\left|\int \tilde{U}(\Omega)\exp\{izk(\Omega)\}\tilde{U}(\omega-\Omega)\exp\{izk(\omega-\Omega)\}d\Omega\right|^2 \qquad (3)$$

where z is the glass thickness and $k(\Omega)$ is the frequency-dependent wavenumber of the glass. This simple SHG model assumes that the nonlinearity has infinite bandwidth, or at least that the spectral response is flat in the region of interest, which is seldom the case for pulses in the few-cycle regime and under normal experimental conditions. Fortunately the resulting SHG power spectrum is still well described by this simple model, provided that a spectral filter is included [28, 29].

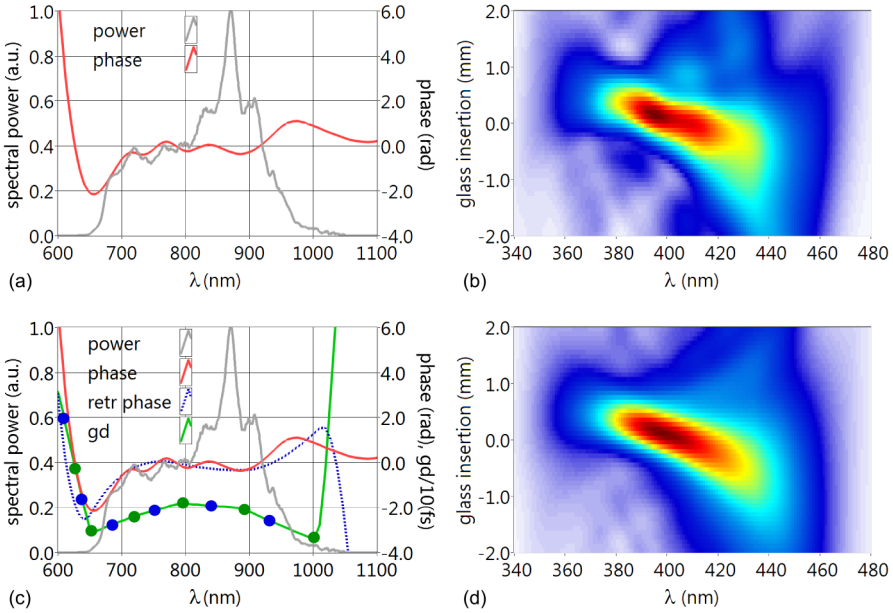

Fig. 1. Measured spectrum and simulated phase (a) and corresponding d-scan trace (b). The algorithm uses a GD representation to try to match the simulated trace (d) to the target trace (b). It starts with a coarse representation which is then interpolated to a finer one as the algorithm reaches a minimum. In (c) a given amount of free parameters are available (green dots), the GD curve is interpolated from those values, and the phase (blue dotted line) is calculated from that GD curve. For this amount of points the best it can do is to produce trace (d). The algorithm then continues by adding more degrees of freedom (blue dots), until it reaches the sampling limit. The previously determined values are still allowed to vary.

Our method consists on measuring the fundamental power spectrum and guessing the spectral phase that reproduces the measured SHG trace, $S(\omega,z)$. As in our previous work [26], we use a general minimization technique (Downhill Simplex [30]), but different basis sets are used to describe the phase. In the original algorithm we used a Fourier series to represent the phase, with the different coefficients of the Fourier series being the optimization parameters. This worked well in most cases but was not enough for others. A simple way to avoid the algorithm getting stuck in local minima is to switch basis whenever this happens: often, a local minimum in a given basis is not a local minimum in another basis, so the simple switching of basis can be a great improvement. For the work presented here, we used several different representations. A good tradeoff between accuracy and speed was obtained by defining the GD values at a given resolution and using spline interpolation in between (similarly to [31, 32]). As the algorithm converges, the resolution is then increased by adding more degrees of freedom. A schematic representation of the algorithm is depicted in Fig. 1, showing an intermediate step of the algorithm while using GD values as a set to represent the guessed phase. The same was done using phase and GDD representations instead of GD values, and switching between those representations whenever the algorithm stalled.

#167354 - $15.00 USD Received 25 Apr 2012; revised 25 May 2012; accepted 12 Jun 2012; published 1 Aug 2012

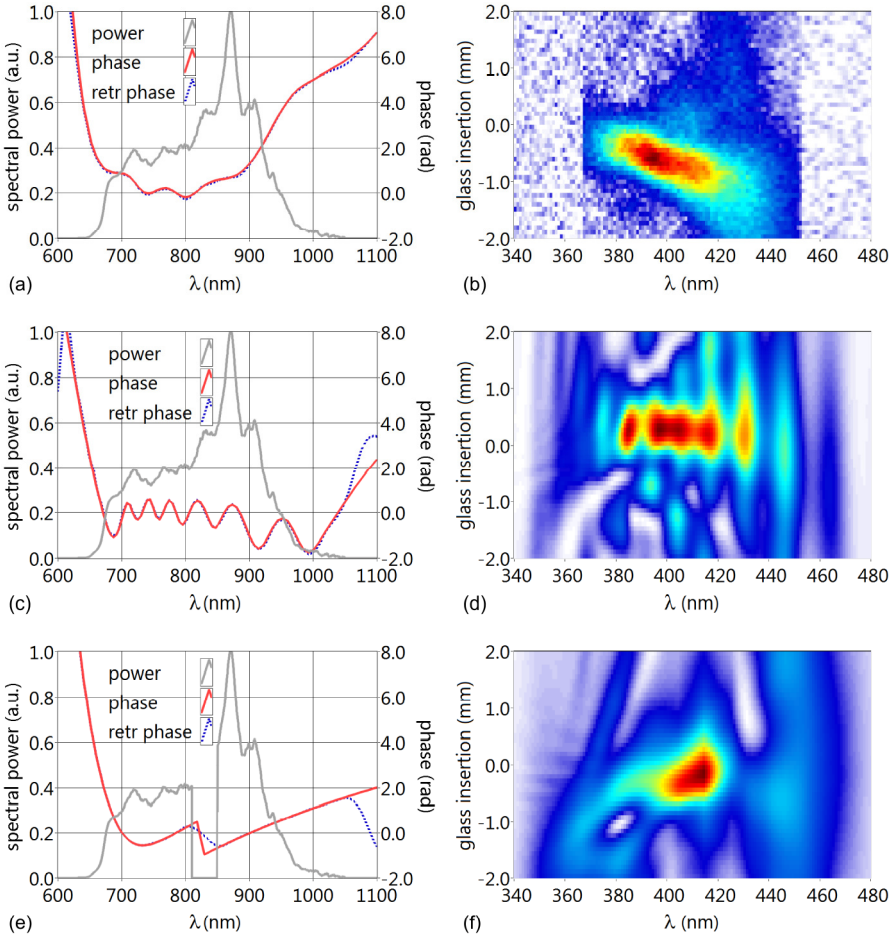

Fig. 2. Example of simulated dispersion scans for different complex cases, where the spectral phase plots on the left correspond to zero insertion in the scans on the right. (a) simulated and retrieved phase and corresponding d-scan (b) multiplied by a crystal response curve, together with hard clipping at the spectral edges and 5% additive noise added. (c) and (d) correspond to relatively small but fast phase variations that heavily distort the trace. (e) and (f) demonstrate the case of a hard-clipped spectrum with phase, group delay and group delay dispersion discontinuities between the resulting two spectral regions. For all of these cases the retrieved phase is in very good agreement with the initial simulated phase.

In previous work we showed that the d-scan method doesn't require an intensity-calibrated SHG signal, and the spectral filter can be retrieved at the same time as the fundamental spectral phase. This is accomplished by using a wavelength-dependent (local) error as the merit function for the minimization algorithm [26].

3. Examples

We briefly study the performance of the method for three different scenarios: measurement noise, strong phase modulation, and spectra with well-separated frequency components (Fig. 2). A d-scan trace is simulated for each different scenario, and the retrieval algorithm is run. In all cases, the "zero" glass insertion on the right side scans corresponds to the shown spectral phase on the left side plots. The fundamental spectrum is an actual measurement from the ultrafast oscillator used in our previous work [26].

#167354 - $15.00 USD Received 25 Apr 2012; revised 25 May 2012; accepted 12 Jun 2012; published 1 Aug 2012

3.1 Noise

A systematic analysis to noise tolerance of a given method invariably involves choosing a "representative" pulse, physically simulating the measurement process, adding noise, and trying to retrieve the original pulse. Given the amount of parameters available, and that each measurement technique has its strengths and weaknesses, it is just too easy to find a case where a given method is superior to others with respect to noise. In view of this, we will not be comparing the d-scan technique to other methods but will simply illustrate qualitatively the tolerance to noise using a "representative" example. For this we simulated a d-scan, applied a spectral filter and added Gaussian noise, with a standard deviation equal to 5% of the peak value of the trace. Even under such unfavorable conditions the retrieved phase is still in very good agreement with the original simulated phase, as seen in Figs. 2(a) and 2(b).

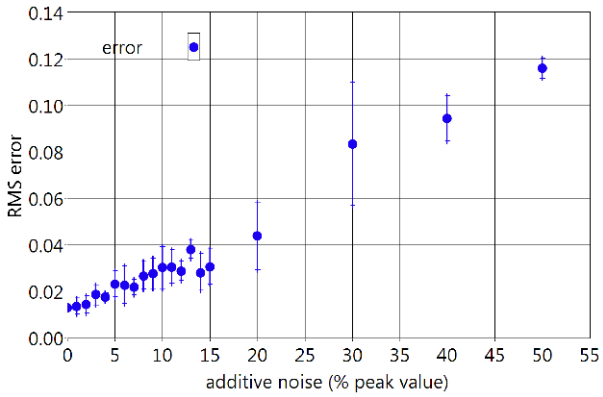

Fig. 3. Error as a function of the added Gaussian noise for the example from Fig. 1(a). For each amount of noise, five retrievals were done. The error bars indicate the standard deviation.

The finer details in the trace will naturally be the first to become "buried" under the noise. Still, even a very noisy signal is often enough to get an estimate of the degree of compression being achieved, since the trace's tilt gives direct indication of uncompensated third and higher order dispersion. This is a very useful feature for real-life situations.

Using the RMS electric field error as defined in [33],

$$\varepsilon = \left\| U_1 - U_2 \right\| = \left[\frac{1}{2\pi} \int \left| \tilde{U}_1(\omega) - \tilde{U}_2(\omega) \right|^2 d\,\omega \right]^{1/2}, \qquad (4)$$

it is possible to study how much the retrieval degrades compared to a noiseless trace for our "representative" pulse (Fig. 3). With the example from Fig. 1(a), with full bandwidth, an RMS noise below 0.02 is readily achievable for a noiseless trace and doesn't appreciably increase up to a noise fraction of about 2%. Then it scales approximately linearly with the added noise, and a retrieval is typically acceptable (RMS error of 0.1) with noise levels as high as 30% of the trace's peak value. It should be pointed out that this depends on many parameters, like the number of samples, scanning range, and the test pulse. The fundamental spectrum is also assumed to be measured without any error.

3.2 Strong phase modulation

Dealing with complex pulses (i.e., pulses with a rapidly varying spectral phase) is a challenging task for all measurement methods [34]. A particularly difficult (and common) situation appears when the generation and/or compression process relies on nonlinear processes like SPM and self-steepening. This increases the time-bandwidth product (TBP) of the pulses, putting higher demands on spectrometer resolution, and increasing the delay range requirements in FROG measurements. Our method makes no assumption about a slowly varying phase, so there isn't in principle a limit for how fast and strong these can be. There

#167354 - $15.00 USD Received 25 Apr 2012; revised 25 May 2012; accepted 12 Jun 2012; published 1 Aug 2012

are some practical issues that should be taken into account though: in our case, the spectral resolution requirements increase both for structured spectral power and phase, as necessary to properly sample each spectrum of the scan. In these conditions, the signal is spread over a larger glass insertion scale, therefore increasing the necessary dispersion scanning range. The retrieval time also increases, as a finer spectral sampling is needed, and more parameters are also needed to properly describe the phase. For the case of SPIDER, provided the signal is well sampled, the direct, non-iterative algorithm is quite insensitive to this added complexity.

Figures 2(c) and 2(d) show an example of a trace for a spectrum with a strongly modulated, rapidly varying phase. Our simulations show that, as long as most of the signal is contained within the scanning region, the d-scan method performs well. As with other techniques, very fast and small phase structures might go unnoticed: experimentally, the spectra are resampled to a grid with a reasonable amount of points to keep computational effort low. If not done carefully (i.e., properly sampling all spectra), this might wash out fine details.

3.3 Spectra with well-separated frequency components

It is often difficult to measure the relative phase between spectral components when there is a gap between them. The fundamental limitation in our technique is similar to all other self-referenced methods [27]. Given two well-separated fundamental frequency components, the trace will contain a signal at the corresponding doubled frequencies, and in addition there will be a cross-term, like in the FROG technique. If this cross-term is broad enough to connect the separate individual SHG parts, then its shape depends on the relative phase between them, and that phase can in principle be recovered. Otherwise, the signal is still sensitive to the group delay between separate spectral components. In the case of SPIDER, large shears will be necessary to "connect" different spectral regions, but this sacrifices measurement resolution. Multi-shearing techniques allow overcoming this problem [35, 36], at the expense of added experimental complexity.

On Figs. 2(e) and 2(f) such an example is shown, where the spectrum was clipped to zero at around 820 nm. For such situation, the width of the cross-term around 410 nm is large enough (and the gap at 820 nm is small enough) not to pose any problem to the algorithm: it handles well, without any modification, discontinuities in the phase, group delay, and group delay dispersion.

All the mentioned problems are linked, and there's a tradeoff between all of them, i.e., a complex spectrum will put more demand on the signal-to-noise ratio, and holes in the spectrum will lead to a longer trace, which in turn requires a larger dispersion range, etc. It is therefore difficult (if not impossible) to make a systematic study on a measurement technique without assuming a particular set of conditions. The cases shown here can be considered "worst case scenarios" within realistic conditions one would usually find in the lab.

4. Experimental results

Two different systems have been characterized for this work. The first is a recently built few-cycle ultrafast laser oscillator, and the second is the output of a hollow fiber compressor. Characterizing such systems is a difficult task for different reasons: in the first case, besides the broad bandwidth, the spectral power is very low at certain wavelengths. In the second case, the spectral power and phase can both be, in some situations, rather complex, due to the nonlinearities involved in the spectral broadening process.

The experimental setup is very similar to the setup described in previous work [26], and consists of a standard pulse compressor made with broadband double-chirped mirrors (IdestaQE, 600-1200 nm bandwidth, GDD ≈-85 fs^2 per bounce at 800 nm) and BK7 glass wedges (Femtolasers GmbH), followed by a focusing off-axis silver parabolic mirror and a SHG crystal (Fig. 4).

In all cases, a full d-scan measurement typically takes a few seconds to perform, and a retrieval can take between a few seconds to a few minutes on a standard personal computer, depending on the complexity of the trace. Both the fundamental and SHG spectra were

#167354 - $15.00 USD Received 25 Apr 2012; revised 25 May 2012; accepted 12 Jun 2012; published 1 Aug 2012

resampled to a 256-point linear array, as this was enough to properly sample the spectra. Between 50 to 60 spectra were acquired for each scan. Depending on the system being characterized, minor changes to the setup were done, as described in the following sections.

4.1 Ultrafast oscillator

The home-built Kerr-lens modelocked laser oscillator used in this section will be described in detail elsewhere [37]. This oscillator presents a challenging case due to its broad and structured spectrum. For SHG, both 5 μm and 20 μm thick BBO crystals (cut for type I SHG at 800 nm) were used in different measurements in order to experimentally investigate the relative insensitivity of the d-scan technique to crystal phase-matching bandwidth [26]. The SHG signal was filtered from the fundamental using a colored highpass filter and a lens was used to collect the signal into a fiber-coupled visible-uv spectrometer (Scansci ScanSpec). The energy per pulse was about 1nJ, at 80 MHz repetition rate.

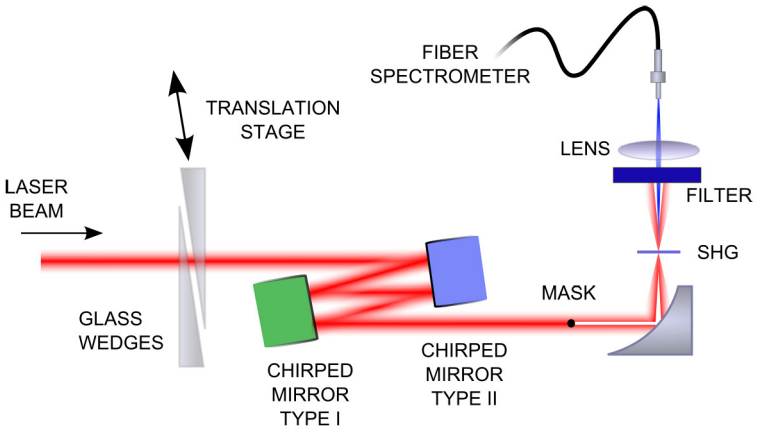

Fig. 4. Experimental setup. The glass wedges are made of BK7, and the chirped mirrors are made in matched pairs to minimize phase ringing. In some cases a mask was used to spatially separate the SHG signal from the fundamental beam at the detector, while in others a blue filter was used to block the fundamental beam (see text). The SHG crystal was either a 5 or 20 μm thick BBO.

Figure 5 shows a comparison between measurements and retrievals made using both crystals. The raw d-scan trace obtained with the 5 μm crystal (Fig. 5(a)) shows a smaller signal-to-noise ratio compared to the 20 μm trace (Fig. 5(f)) due to lower SHG conversion efficiency in the thinner crystal, but also features a larger relative signal in the longer wavelength side due to the larger phase matching bandwidth. The calibrated scans (Figs. 5(b) and 5(g)), obtained by applying the calibration curve given by the d-scan retrieval algorithm to the measured (raw) d-scan traces, are very similar in both cases, apart from the expected higher signal-to-noise ratio for the thicker crystal. For each crystal, five different data sets were used on five different retrievals, allowing us to perform a statistical analysis and to estimate the confidence levels of the result.

#167354 - $15.00 USD Received 25 Apr 2012; revised 25 May 2012; accepted 12 Jun 2012; published 1 Aug 2012

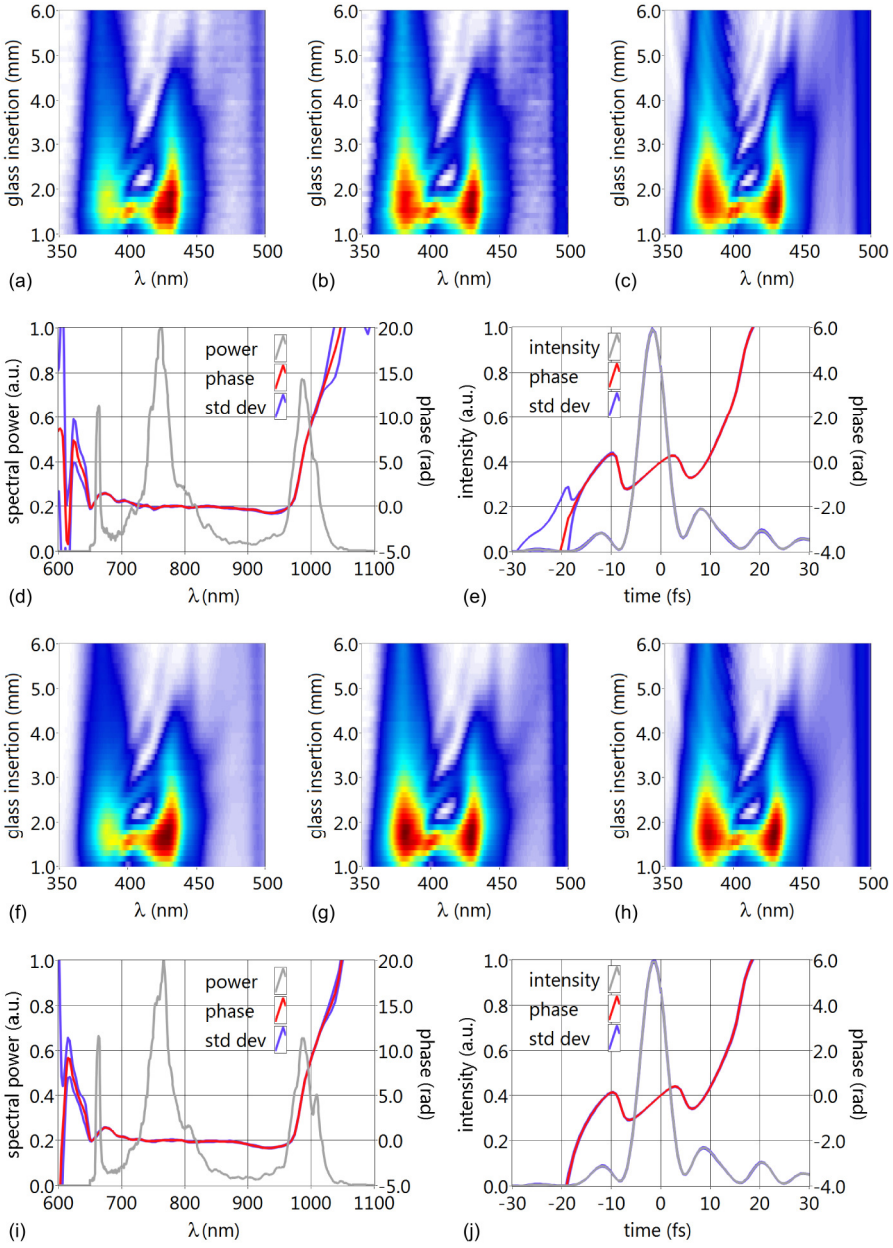

Fig. 5. Measured (a), calibrated (b), and retrieved (c) scans from the home-built ultrafast oscillator, obtained with a 5 μm thick BBO crystal. The retrieved phase statistics in the spectral domain (d) and the corresponding time reconstructions (e) were obtained from 5 different measurements and retrievals. The same applies to plots (f) to (j), but for a 20 μm thick crystal. The measured pulse duration is 6.0 ± 0.1 fs FWHM, with a Fourier limit of 5.2 fs for both cases.

In both cases, the shortest pulse duration obtainable for this chirped mirror set and glass combination was 6.0 ± 0.1 fs FWHM, achieved for a glass insertion of 1.5 mm. The Fourier limit for both spectra is 5.2 fs FWHM.

#167354 - $15.00 USD Received 25 Apr 2012; revised 25 May 2012; accepted 12 Jun 2012; published 1 Aug 2012

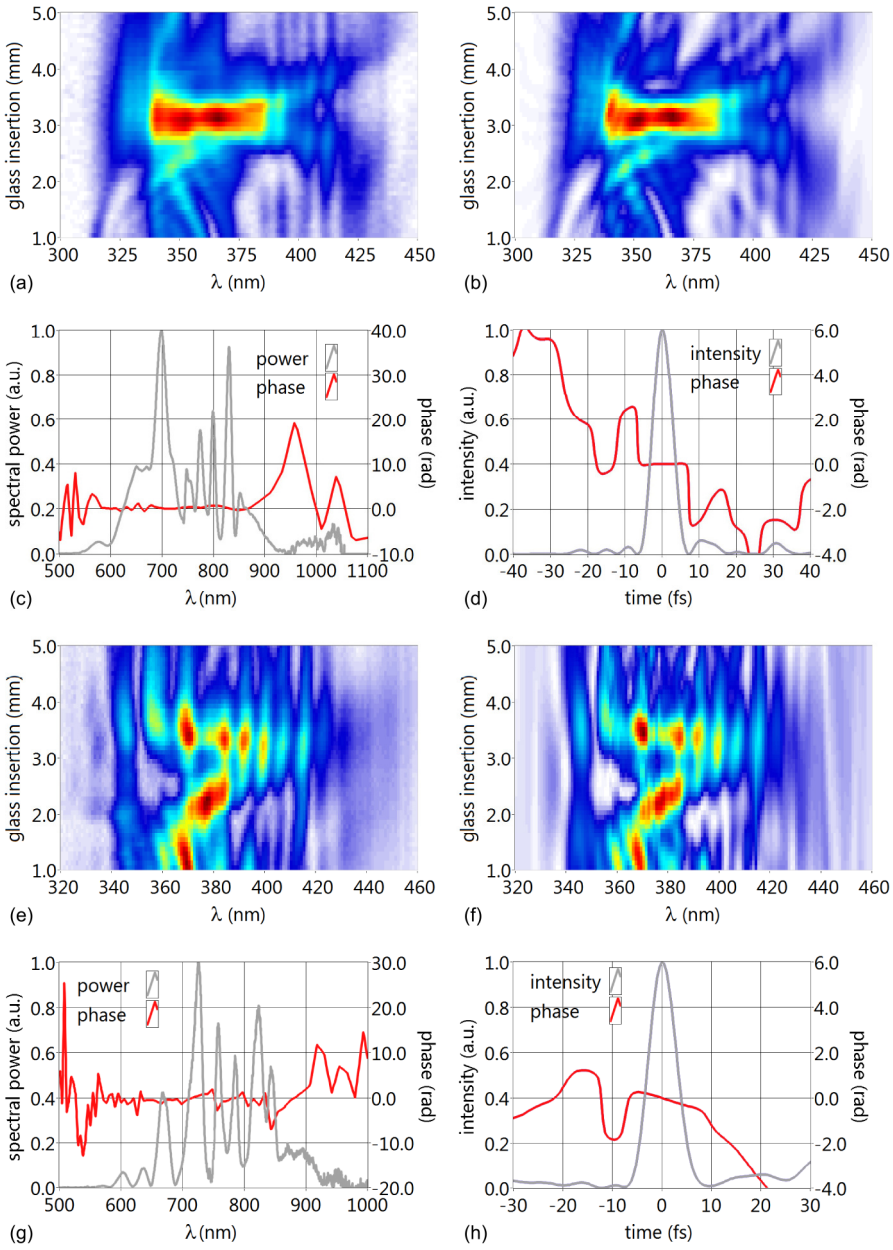

Fig. 6. Measured (a) and (e), and retrieved (b) and (f) scans from a hollow-fiber compressor operating in different regimes. The measured pulse durations are respectively 6.2 and 6.5 fs FWHM, with Fourier limits of 4.7 and 6.1 fs.

Due to UV absorption in the glass filter, the expected SHG signal at around 330 nm (corresponding to the peak at around 660 nm in the fundamental spectrum) is absent from our measurements. This (weak) signal is nevertheless present in the retrieved traces (not shown), which also shows that the phase from that spectral region is encoded in the remaining of the trace. A similar argument holds regarding the peak at 1000 nm: the corresponding SHG signal at around 500 nm varies very little across the insertion scale, thus yielding little information about the fundamental spectral phase; yet, that phase strongly shapes the trace around the 360 to 460 nm region, which allows it to be determined. The fact that all retrievals give very

#167354 - $15.00 USD Received 25 Apr 2012; revised 25 May 2012; accepted 12 Jun 2012; published 1 Aug 2012

similar results, independently of factors such as first guesses for the algorithm, chosen basis, etc., further reassures us of the accuracy of the retrievals.

4.2 Hollow-fiber

For the case of ultrashort pulses obtained from spectral broadening in gas-filled hollow-core fibers, the nonlinear processes inherent to the broadening process are responsible for fast and strong oscillations on both spectral power and phase. Different operating conditions that depend on many parameters such as alignment, input power, beam size, etc., might lead to very different spectral structures. We characterized the output of a hollow fiber compressor under two different operating conditions: in the first one, the fiber was aligned so as to get a spectrum as broad as possible, while in the second case it was aligned so as to optimize the quality of the spatial profile of the output beam.

The hollow fiber used had a 250 μm inner diameter, was filled with approximately 500 mbar of Argon, and pumped with 800 μJ, sub-30 fs pulses from a 1 kHz Ti:Sapphire amplifier (Femtolasers FemtoPower Compact PRO CEP). For SHG we used a 5 μm thick BBO crystal.

The output of the fiber usually has measurable spectral wings down to 300 nm. While much weaker than the main spectral part, this is still enough to prevent proper measurement of the SHG signal if not properly filtered.

The blue filter used in the previous case (ultrafast oscillator) blocked too much of the SHG signal, as it also absorbed wavelengths shorter than 360 nm. Instead, we opted to block a small central portion of the fundamental beam with a thin wire (the "mask" shown in Fig. 2) and measured the central part of the SHG signal. The resulting spatial separation was enough to eliminate the fundamental signal, without any additional spectral filtering. Both the fundamental and SHG spectra were measured with a broadband fiber-coupled spectrometer (Ocean Optics HR4000).

The results for both operating conditions are shown in Fig. 6. Figures 6(a) to 6(d) correspond to the case where the hollow fiber was optimized for spectral bandwidth, while Figs. 6(e) to 6(h) are for the case where the spatial mode was best.

5. Conclusion

We have successfully demonstrated the applicability of ultrashort pulse characterization by numerical phase retrieval from second-harmonic dispersion scans for cases that are representative of broadband state-of-the-art sources. Compared to our previous work, the phase retrieval algorithm has been improved by swapping the base and/or the representation of the quantity being retrieved (phase, GD, GDD) whenever calculations would stall. The technique proved to be robust with respect to spectral complexity (power and phase), noise, and bandwidth limitations, not only in simulations but in real laboratory conditions as well. Measurements performed on a home-built broadband few-cycle laser oscillator using two nonlinear crystals of different thicknesses (5 μm and 20 μm) resulted in the same retrieved pulse profile and duration (6.0 ± 0.1 fs FWHM) in spite of the different phase matching bandwidth conditions and signal-to-noise ratios of the corresponding traces. Few-cycle pulses with complex and highly modulated spectra generated by a hollow-fiber compressor under two different alignment conditions (broadest spectrum and best spatial profile) were also successfully retrieved with this technique (6.2 and 6.5 FHWM, respectively).

The main drawbacks of this method are its iterative nature (there is the possibility that the algorithm gets stuck during minimization) and, in its current implementation, its intrinsic multi-shot nature. It is also based on a 1D model, so space-time coupling effects are not presently taken into account.

In principle there is no reason why this method shouldn't work down to the single-cycle regime. The fact that most of the fundamental phase information is contained within the cross-terms clearly makes the technique very tolerant with respect to bandwidth limitations regarding SHG generation and detection. The intrinsic simplicity (most of the experimental

#167354 - $15.00 USD Received 25 Apr 2012; revised 25 May 2012; accepted 12 Jun 2012; published 1 Aug 2012

setup is actually a standard chirped mirror compressor similar to those already existent in many laboratories) and ease of alignment are also some of the most attractive features of this method.

Acknowledgments

This work was partly supported by FCT – Fundação para a Ciência e a Tecnologia and FEDER (grants SFRH/BD/37100/2007, SFRH/BD/69913/2010, PTDC/FIS/115102/2009 and SFRH/BSAB/1100/2010), the ESF - European Science Foundation ("Super-intense laser-matter interactions" grant 4596), grant program Formación de Profesorado Universitario (Benjamín Alonso), Ministerio de Ciencia y Tecnología, Subdirección General de Proyectos de Investigación (Project FIS2009-07870), the European Research Council (ALMA), the Marie Curie Intra-European Fellowship ATTOCO, the Marie Curie Initial Training Network ATTOFEL, the Knut and Alice Wallenberg Foundation, the Joint Research Programme ALADIN of Laserlab-Europe II and the Swedish Research Council. The authors would like to thank Adam Wyatt for valuable comments and insight, and to Scansci for the kind loan of a vis-uv spectrometer.

#167354 - $15.00 USD Received 25 Apr 2012; revised 25 May 2012; accepted 12 Jun 2012; published 1 Aug 2012